Fibers and Polymers 2013, Vol.14, No.4, 578-583 DOI 10.1007/s12221-013-0578-5

Electrospun Poly(L-lactic)Acid/Nanoalumina (PLA/Al_2O_3) Composite Fiber Mats with Potential Biomedical Application - Investigation of Cytotoxicity

P. Kurtycz*, T. Ciach[1], A. Olszyna, A. Kunicki[2], E. Radziun[3], M. Roslon[3], J. Dudkiewicz-Wilczynska[3], K. Nowak[3], and E. Anuszewska[3]

Faculty of Materials Science and Engineering, Warsaw University of Technology, 02-507 Warsaw, Poland
[1]*Faculty of Chemical and Processing Engineering, Warsaw University of Technology, 00-645 Warsaw, Poland*
[2]*Faculty of Chemistry, Warsaw University of Technology, 00-664 Warsaw, Poland*
[3]*Department of Biochemistry and Biopharmaceuticals, National Medicines Institute, 00-725 Warsaw, Poland*
(Received June 22, 2012; Revised September 3, 2012; Accepted September 9, 2012)

Abstract: PLA fibrous mats containing nanoalumina filler were fabricated by electrospinning method. The morphology of the mats was characterized by SEM, and TEM. In vitro biocompatibility of the electrospun fiber mats was also evaluated. Indirect cytotoxicity evaluation of the fiber mats with human skin fibroblasts revealed that the materials were non-toxic to living cells. The cells cultured on the fibrous mat exhibited normal cells shapes and were integrated well with surrounding fibers. The obtained results confirmed the potential for use of the electrosupun PLA/Al_2O_3 fiber mats for biomedical application.

Keywords: PLA, Alumina, Electrospinning, Cytotoxicity, Fiber mats

Introduction

Electrospinning is a very promising and very interesting method of fibers production. This technique allows producing fibers of a diameter ranging from few nanometers up to 1 mm [1]. Electrospining has been proven as a novel and effective method to produce such fibrous structures [2-4]. Electrospinning possesses great advantages, such as simplicity of use, adaptability and versatility in spinning a wide variety of polymeric fibers [5]. Recently this technique has been recognized as an efficient method to produce nanoscale fibrous structures, and electrospun PLA based nanofiber mats have attracted a great deal of attention due to their potential applications in drug delivery, prevention of post-surgery adhesion and biometic scaffolds for tissue engineering [6-8]. Nanofibers formed by electrospinning have been shown to mimic the extracellular matrix (ECM) environment to various degrees when cultured with several cell types [9-11]. Incorporation of particles into electrospun fibers was repeatedly reported for inorganic nanoparticles such as hydroxyapatite for bone tissue engineering [12] or silver for use antibacterial wound dressing [13]. Nanofibrous organic and inorganic composite scaffolds containing nano-sized demineralized bone powders with biodegradable PLA by electrospinning, which may serve as favorable matrix for the regeneration of bone tissue [14]. Alumina is one of the most important ceramics for structural applications. Furthermore, it also exhibit excellent biocompatibility and bone-bonding [15-17]. Decreasing grain sizes have been shown to improve the hardness and wear resistance [18]. Nanoalumina has no cytotoxity effects on the human skin fibroblasts (BJ) [19]. Polylactide (PLA) is polyester produced by lactide ring-opening polymerization process. PLA has been the focus of significant research over the past 40 years and has long track record of clinic application due to its biodegradability, biocompatibility, good mechanical properties [20,21] decompose over a period of time [22] and ability to be dissolved in common solvents for processing [20,21]. Products of its decomposition are charmless and are metabolised by the organism. A basic requirement of scaffolds is sufficient mechanical strength which provides an adequate stability of the scaffolds. The mechanical properties fibers are important parameters in tissue engineering. The purpose of a scaffold is not only for providing a surface for cell residence but also for maintaining mechanical stability at the defect site of the host [23]. A well-designed tissue engineered scaffold has to meet two mechanical requirements to be effective. The scaffold must retain structural integrity and stability when a physician handles and implants it into the defect site of the host. And after surgery, the structure at the implant site must provide sufficient biomechanical support during the process of tissue regeneration and structure degradation.

The aim of this paper is to put in evidence the potentiality of emergent nanocomposite approaches in tissue engineering applications. Moreover, in-vitro cytotoxicity of the nanocomposite fiber mats on the human skin fibroblasts (BJ) are discussed.

Experimental

Synthesis of the Alumina Nanopowder

For alumina synthesis we have used the process that has been described and claimed by us earlier [24,25]. It consists of reaction of aluminum organometallic compound and alumoxane with oxygen, provided in organic solvent.

*Corresponding author: patrycja.kurtycz@gmail.com

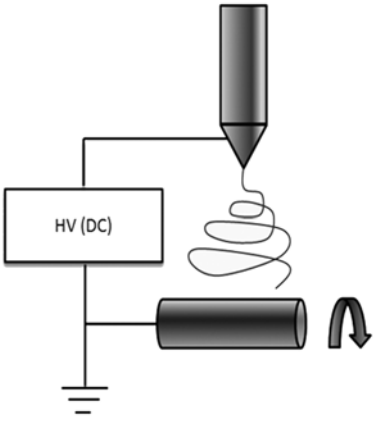

Figure 1. Schematic of the electrospinning method.

Fabrication of Nanofiber Mats

The poly(L-lactic)acid (PLA; molecular weight, Mw: 220 kDa; Mn: 101 kDa) was obtained from Biomer, Krailing, Germany (product name Biomer L9000) was stirred for 1 day in $CHCl_3$/EtOH (1.5/1 v/v) solution. In the next step nanopowder Al_2O_3 was added (none, 1, 5, 10 wt.% based on the weight of the PLA), and stirred for 1 hour. Then, the nanocomposite fibers were produced by electrospinning method using the setup depicted in Figure 1. The applied voltage was 18 kV, liquid flow was set at 1 ml/h and was forced by the medical syringe pump. As a spraying nozzle blunt epidermic needle (18G) of 1 mm inner diameter was applied. The fiber collecting drum diameter was 20 mm, and the distance between the nozzle and the drum was 15 cm. Drum rotated at approximately one revolution per second.

Characterization of Substrates and Fiber Mats

The morphological aspect of the PLA/Al_2O_3 nanocomposite fibers as well as Al_2O_3 nanopowder, used in PLA/Al_2O_3 nanocomposite fiber production process, was investigated by electron microscopy (SEM, Zeiss LEO 1530) operating at 2.0 kV. For microscopic investigations fibers were attached to a carbon sticky tape and sputtered with gold. For Al_2O_3 nanopowder observations, a droplet of nanopowder dispersed in 2-propanol was placed onto a thin silicon plate. The plate was then dried and carbon coated using BAL-TEC SCD with CEA 035 attachment.

The average particle size of the Al_2O_3 nanopowder was estimated from a distribution acquired by using stereological methodology [26]. Particles parameters were estimated for their cross-sections and the average value of each parameter was then estimated. All quantitative analysis were performed using the MicroMeter v.086b computer program.

Its Bruanauer-Emmet-Teller (BET) specific surface area was determined using Quadrasorb-SI Quantachrome equipment. Before BET measurements, all samples were degassed in 350 °C for 24 hours. The process of adsorption was provided in −195.8 °C bath and gaseous nitrogen was used as an adsorbate. Also alumina nanopowder was analysed by X-ray diffraction method (PHILIPS PW 1830 with Cu K_α radiation).

The PLA/Al_2O_3 nanocomposite fibers were also examined in a transmission electron microscope (TEM, PHILIPS CM 20) operated in the high-resolution mode, chiefly in order to identify the Al_2O_3 nanoparticles. The TEM photographs were taken in both light and dark fields. The PLA/Al_2O_3 nanocomposite fibers were examined by energy dispersive X-ray spectroscopy (EDS unit coupled with the TEM employed). The analysis gave information about the local contents of the elements present in a given region.

The diameter of fiber mats were measured by optical microscope Nikon Eclipse 80i, and analysis were performed using the NIS-Elements BR 3.00 SP2, Nikon, computer program.

The mechanical properties were carried out on Instron 5566. The fiber mats were prepared in the form of standard dumbbell shapes according to ASTM Standard D 638 and tensile properties were calculated using programme Bluehill 2, version 2.14 from Instron company. The sample was vertically mounted on two mechanical gripping units of the tensile tester at their ends. Deforming speed was set at 10 mm/min. Cross section area of the fiber and the composite

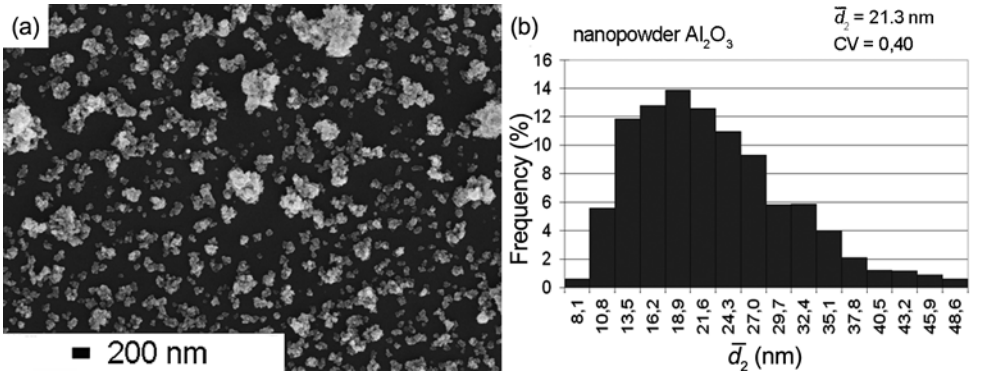

Figure 2. Representative SEM image (a) of the Al_2O_3 nanopowder used in polylactide-alumina nanocomposite fiber production process and (b) and particle size distribution.

specimens was determined using micrometer. An average value of tensile strength was taken from 5 specimens of each composite.

The cells were observed by an invert microscope Nikon Eclipse TS-100/F, in order to assess their morphology and check their overall health after exposure to PLA/Al_2O_3 fiber mats.

In vitro Cytotoxicity of Fiber Mats

Human skin fibroblasts (BJ, ATCC) were cultured and maintained in Eagle's medium (EMEM, Lonza), supplemented with 10 % fetal bovine serum (FBS, Lonza) and 1 % antibiotics (Penicillin-Streptomycin-Amphotericin B, Lonza). The cells were grown as monolayers in T-25 or T-75 culture flask (Nunc). The BJ adherent cell were detached with trypsin-EDTA solution (Lonza) for 2-5 min, resuspended in complete culture medium and counted using Coulter Z2 (Series). For assay, the cells were plated in 96- and 6-well plates, at a density needed to reach at least 80 % confluence. The cell were maintained at 37 °C in the humidified atmosphere with 5 % CO_2.

The fiber mats PLA/Al_2O_3 (1, 5, 10 wt.% based on the weight of the PLA) were cuts for circular discs: 10 mm in diameter and sterilized by UV radiation for 15 minutes on both sides. As a positive cytotoxicity control were used latex discs with 10 mm diameter, and as a negative cytotoxicity control were used circular discs: pure PLA fiber mats.

After preincubation period (48 hours), cultured medium was removed and replaced by new one. For assay, the cells were plated at 8×10^4 (for 24 hours incubation) or 6.6×10^4 (for 48 hours incubation) cells/ml. Circular discs: PLA/Al_2O_3 (1, 5, 10 wt.% based on the weight of the PLA), latex and pure PLA, was added and cells were incubated for 24 and 48 hours at 37 °C, in a 5 % CO_2.

MTT Assay (Quantification of viable cells)

The MTT assay is based on the fact that metabolically active cells interact with a tetrasolium salt in an MTT reagent to produce a soluble formazan dye, which absorbs light at the wavelength of 540 nm. The intensity of the absorbance is proportional to the number of viable cells.

After 24 or 48 hours of exposure to different circular discs PLA/Al_2O_3 (1, 5, 10 wt.% based on the weight of the PLA), latex and pure PLA, the medium was removed and each well was rinsed by 1 m*l* phosphate buffered saline (PBS) without Ca^{2+} and Mg^{2+}. Then 750 μl of 5 mg/m*l* MTT solution (Thiazolyl blue tetrazolium bromide, AppliChem) was added into each well and incubated for 4 h at 37 °C, in a 5 % CO_2. The obtained violet color formazan crystals were dissolved in 3 m*l* 99,7 % isopropyl alcohol (Rathburn Chemicals),and 250 μl of solution was removed to 96-well plates and the absorbance of each well was measured using a microplate reader (iEMS Reader MF) at 540 nm.

Statistical Analysis

MTT assays for all cell lines were repeated in three independent experiments. All data were expressed as mean ± standard deviation (SD). Statistical analysis was performed using the SYSTAT 13 software (ver. 13.00.05; Systat Software Inc., USA). F-Snedecor's test for equality of variances and unpaired Student's t-test adjusted for both equal and unequal variances to estimate the equality of means were applied for groups comparison at significance level a=0.05.

Results and Discussion

Characteristic of the Fiber Mats PLA/Al_2O_3

The representative SEM image of the alumina nanopowder and particle size distribution, is presented in Figure 2. The figure and particle size distribution clearly demonstrates the formation of single nanoparticles with average particle size 21.3 nm. Specific BET surface area of the nanoalumina was 219.3 m^2/g. The specific surface area (exceeds 200 m^2/g) with a great number of open pores (above 1.9 cm^3/g), which gives evidence that their tendency to agglomeration is only slight and that the possible agglomerates have a loose structure. The X-ray diffraction pattern corresponding to the alumina nanopowder is shown in Figure 3. As it can be observed, peaks corresponding to gamma and eta alumina phase are present.

The representative SEM images of the polylactide-alumina nanocomposite fibers containing different amounts of Al_2O_3 (0, 1, 5, 10 wt.% based on the weight of the PLA) are presented in Figure 4. As can be seen, fibers are loosely arranged in the analyzed area. Adding 5 or 10 wt.% of the Al_2O_3 filler results in the most visible changes in the PLA structure (Figure 4(c),(d)). Clearly visible changes are present on the fiber surface structure, which is not as smooth as the surface of pure PLA fiber (Figure 4(a)). The formation of single nanoparticles with average particle size was 21.3 nm, resulting in good incorporation into PLA fibers.

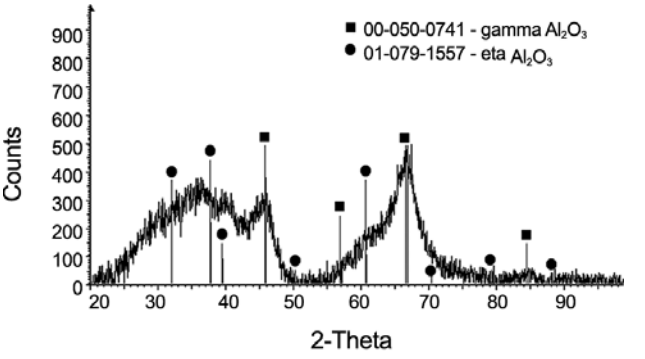

Figure 3. Representative X-ray diffractogram of the Al_2O_3 nanopowder used in polylactide-alumina nanocomposite fibers production process.

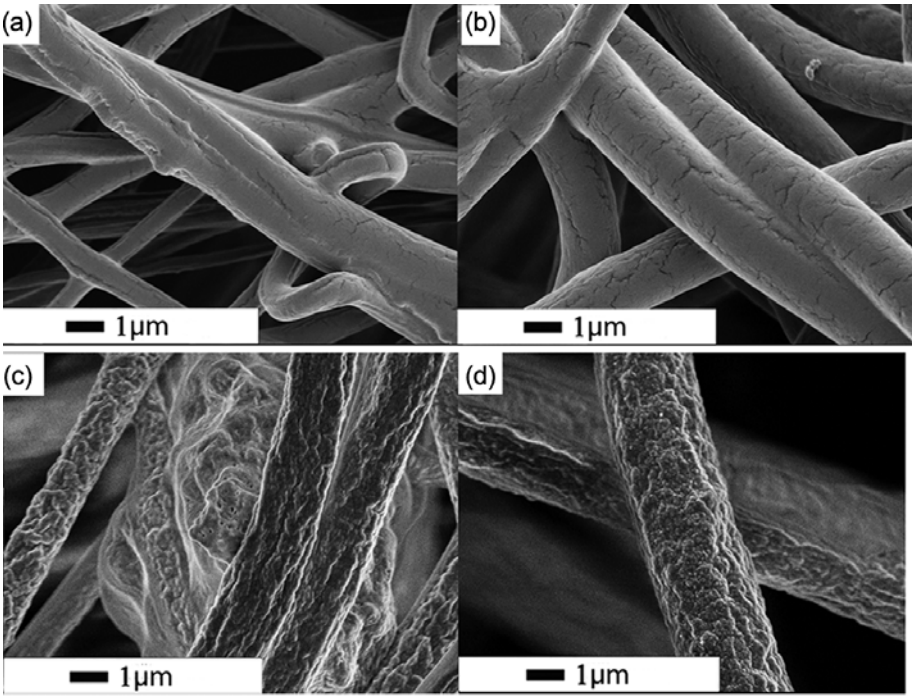

Figure 4. Representative SEM images of the (a) pure PLA, (b) PLA with 1 wt.% Al_2O_3, (c) PLA with 5 wt.% Al_2O_3, and (d) PLA with 10 wt.% Al_2O_3.

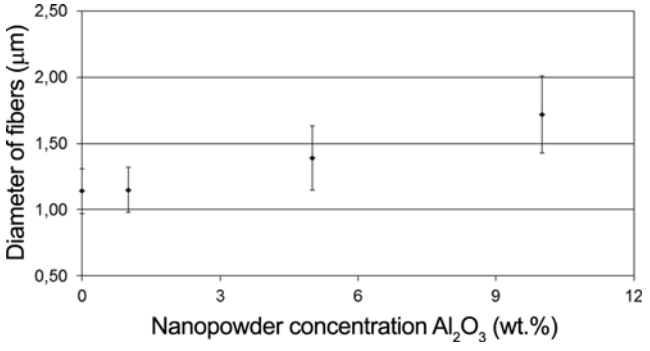

Figure 5. Influence of Al_2O_3 nanopowder concentration on the diameter of fibers.

The diameters of the PLA/Al_2O_3 nanofiber mats with 0, 1, 5, 10 wt.% of Al_2O_3 were 1.14, 1.15, 1.39, 1.72 μm, respectively (Figure 5). The alumina nanoparticles have an effect on the formation of thicker PLA nanofibers.

The PLA-Al_2O_3 nanocomposite fibers were also examined in a transmission electron microscope (TEM). Figure 6 shows a TEM image (taken in the dark field) obtained for the PLA/Al_2O_3 (10 wt.% Al_2O_3) nanocomposite fibers. The TEM of PLA fibers on Al_2O_3 indicates the surface dispersion ratio of alumina element. The Al_2O_3 nanoparticles are uniformly distributed with an average size of 21.3 nm and a few particles Al_2O_3 seem to aggregate to some extent. In Figure 6(b), (measurement made at point marked O1 in Figure 6(a)) we can observed peaks corresponding to aluminum, oxygen and carbon. In Figure 6(c), 6(d), 6(e) (measurement made at point marked O2, O3 and O4 in Figure 6(a), respectively), we can observed peaks corresponding to the same elements as in Figure 6(b). This is proof that the fibers are composites.

Tensile test were performed to determine any changes in mechanical properties because of alumina nanopowder concentration of 0, 1, 5, 10 wt.%. The results are shown in Figure 7. Tensile nanocomposite fibers showed the maximum tensile strength (about 0.5 MPa) for the fiber mats with 1 and 5 wt.% of Al_2O_3. The sample with 10 wt.% of Al_2O_3 had less tensile strength, but still higher than pure PLA fiber mats. This may be attribution of agglomeration nanopowder at the higher concentration, which could limit the effective surface area available for load transfer. The general, the mechanical properties of PLA/Al_2O_3 composites fibers are better than pure PLA fibers.

Cytotoxicity Effects of the PLA/Al_2O_3 Nanocomposites

The MTT assay is based on the fact that metabolically active cells interact with a tetrasolium salt in an MTT reagent to produce a soluble formazan dye. The intensity of the absorbance is proportional to the number of viable cells. BJ cells viability after exposure and incubation with the test fiber mats are illustrated in Figure 8. Observation on microscope shows good results (shape, size) for cells BJ after 24 and 48 hours of exposure to tested fiber mats.

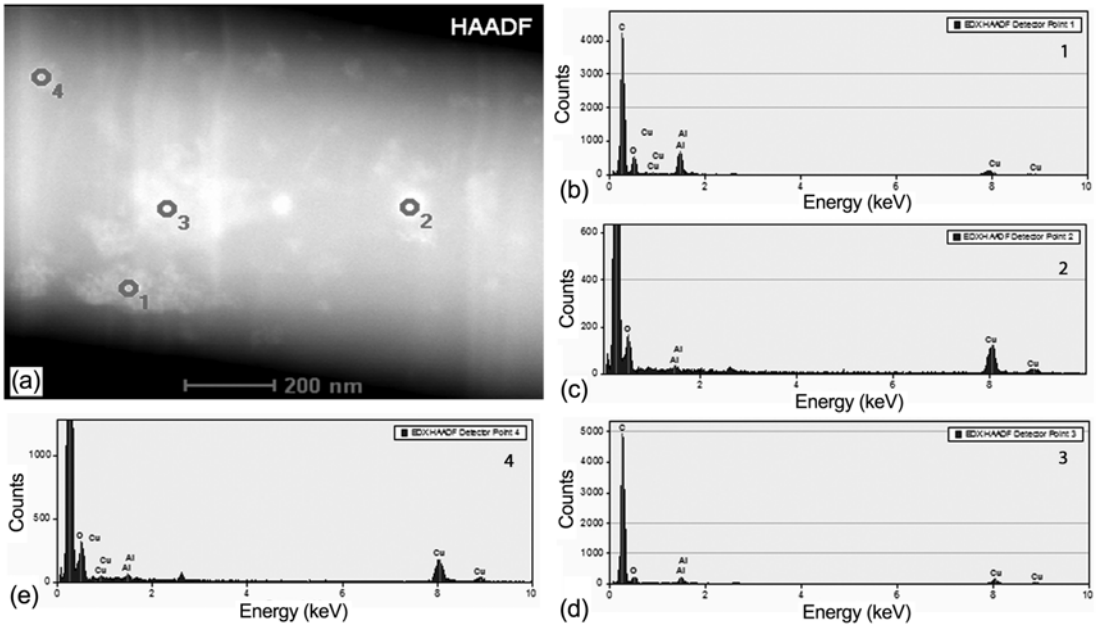

Figure 6. Representative TEM images of PLA-Al_2O_3 fibers (a), and EDS results (b) at point 1, (c) at point 2, (d) at point 3, and (e) at point 4.

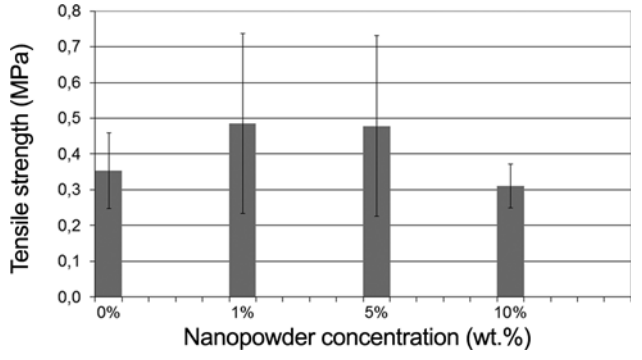

Figure 7. Mechanical properties of fiber mats PLA/Al_2O_3.

The results obtained for the MTT assay demonstrated that PLA/Al_2O_3 nanocompistes are not cytotoxicity of human skin fibroblast cells, even at concentration Al_2O_3 as high as 10 wt.%. As shown on Figure 9 after 24 hours of exposure to test different fiber mats PLA/Al_2O_3 (none, 1, 5, 10 wt.% based on the weight of the PLA) the human (BJ) fibroblasts viability amounted respectively 101,53 %, 103,28 %, 98,42 % and 97,21 % relative to control. After 48 hours incubation viability amounted: pure PLA – 104,56 %, 1 wt. % Al_2O_3 – 99,41 %, 5 wt.% Al_2O_3 – 106,54 % and 10 wt.% Al_2O_3 – 104,47 %.

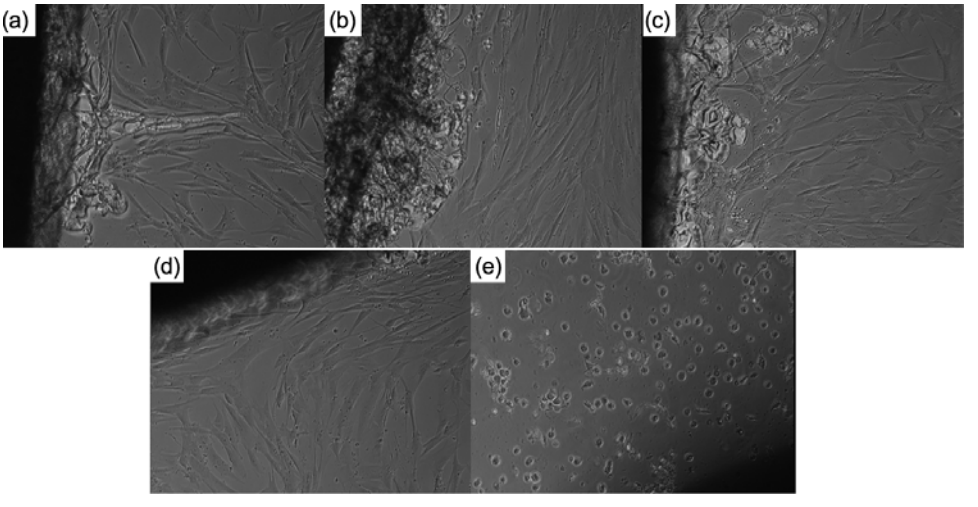

Figure 8. Exemplary photographs of BJ cells, with (a) PLA (negative control), (b),(c),(d) fiber mats PLA/Al_2O_3 (1, 5, 10 wt.% based on the weight of the PLA) and (e) latex (positive control).

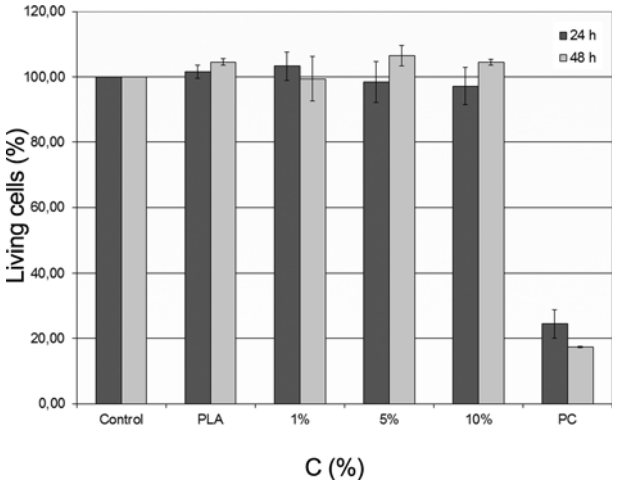

Figure 9. Cytotoxicity profiles of PLA/Al_2O_3 fiber mats, when incubated with human skin fibroblasts (BJ) as determined by MTT assay, (PC-positive control, latex). Percent viability of cells was expressed relative to control cells. Results are represented as mean ± SD.

Conclusion

In the present communication, electrospun PLA/Al_2O_3 fiber mats were prepared form PLA and Al_2O_3 nanopowder in $CHCl_3$/EtOH solution. These fiber mats were evaluated for potential use as biocompatible dressing or scaffolding materials for skin tissue engineering, using human skin fibroblasts (BJ). Indirect cytotoxicity evaluation using BJ as referenced cells indicated that the PLA/Al_2O_3 fiber mats were non-toxic and could be used as biocompatible dressing or scaffolding materials. In addition, the cells cultured on the fibrous mats exhibited normal cell shapes and integrated well with surrounding fibers. Visual observation on microscope showed that the cells maintained their characteristic morphology during the cell culture. Structure of the electrospun fiber mats is favorable parameter for promoting the attachment and the proliferation of the cells [27,28]. Fiber mats PLA/Al_2O_3 showed no significant cytotoxic effects to tested human (BJ) skin fibroblast at tested concentration. However obtained results should be confirmed by further biological research.

References

1. J. Doshi and D. Reneker, *Journal of Electrostatics*, **35**, 151 (1995).
2. P. Wutticharеonmongkol, N. Sanchavanakit, P. Pavasant, P. Supaphol, *J. Nanosci. Nanotechnol.*, **6**, 514 (2006).
3. T. B. Bini, S. J. Gao, T. C. Tan, S. Wang, A. Lim, L. B. Hai, and S. Ramakrishna, *Nanotechnology*, **15**, 1459 (2004).
4. C. A. Bashur, L. A. Dahlgren, and A. S. Goldstein, *Biomaterials*, **27**, 5681 (2006).
5. T. J. Still and H. A. von Recum, *Biomaterials*, **29**, 1989 (2008).
6. X. H. Zong, S. Li, E. Chen, B. Garlick, K. S. Kim, D. F. Fang, J. Chiu, T. Zimmerman, C. Brathwaite, B. S. Hsiao, and B. Chu, *Annals of Surgery*, **240**, 910 (2004).
7. W. G. Cui, X. H. Li, X. L. Zhu, G. Yu, S. B. Zhou, and J. Weng, *Biomacromolecules*, **7**, 1623 (2006).
8. W. J. Li, C. T. Laurencin, E. J. Caterson, R. S. Tuan, and F. K. Ko, *J. Biomed. Mater. Res.*, **60**, 613 (2002).
9. S. M. Mo, C. Y. Xu, M. Kotaki, and S. Ramakrishna, *Biomaterials*, **25**, 1883 (2004).
10. C. Xu, R. Inai, M. Kotaki, and S. Ramakrishna, *Tissue Engineering*, **10**, 1160 (2004).
11. Z. Ma, M. Kotaki, R. Inai, and S. Ramakrishna, *Tissue Engineering*, **11**, 101 (2005).
12. H. Jiang, D. Fang, B. Hsiao, and B. Chu, *J. Biomater. Sci., Polym. Ed.*, **15**, 279 (2004).
13. W. H. Park, W. K. Son, J. H. Youk, and T. S. Lee, *Macromolecular Rapid Communications*, **25**, 1632 (2004).
14. E. K. Ko, S. I. Jeong, N. G. Rim, Y. M. Lee, H. Shin, and B. K. Lee, *Tissue Engineering, Part A*, **14**, 2105 (2008).
15. H. Warashina, S. Sakano, S. Kitamura, K. I. Yamauchi, J. Yamaguchi, N. Ishiguro, and Y. Hasegawa, *Biomaterials*, **24**, 3655 (2003).
16. Y. Takami, T. Nakazawa, K. Makinouchi, J. Glueck, and Y. Nose, *J. Biomed. Mater. Res.*, **36**, 381 (1997).
17. K. Rezwan, Q. Z. Chen, J. J. Blaker, and A. R. Boccaccini, *Biomaterials*, **27**, 3413 (2006).
18. A. Krell, *Mater. Sci. Eng.*, **A209**, 156 (1996).
19. E. Radziun, J. Dudkiewicz Wilczynska, I. Ksiazek, K. Nowak, E. L. Andruszewska, A. Kunicki, and A. Olszyna, *Toxicology in vitro*, **25**, 1694 (2011).
20. T. Nakamura, S. Hitomi, S. Watanabe, Y. Shimizu, K. Jamshidi, S. H. Hyon, and Y. Ikada, *J. Biomed. Mater. Res.*, **23**, 1115 (1989).
21. P. U. Rokkanen, O. Bostman, E. Hirvensalo, E. A. Makela, and E. K. Partio, *Biomaterials*, **21**, 2607 (2000).
22. M. Vert, S. M. Li, G. Spenlehauer, and P. Guerin, *J. Mater. Sci.: Mater. Med.*, **3**, 432 (1992).
23. D. W. Hutmacher, *Biomaterials*, **20**, 2529 (2000).
24. A. Solgala, A. Kunicki, and A. Olszyna, *Ceramic Materials*, **60**, 262 (2008).
25. P. Czarnecka, T. Ciach, A. Kunicki, A, Olszyna, M. Gołaszewska, and A. Jastrzebska, *Inzynieria Materialowa*, **3**, 467 (2010).
26. K. J. Kurzydłowski, "The Quantitative Description of the Microstructure of Materials", CRC Press LLC, 1995.
27. M. M. Stevens and J. H. George, *Science*, **310**, 1135 (2005).
28. W. Li, R. Tuli, C. Okafor, A. Derfoul, K. Danielson, D. Hall, and R. Tuan, *Biomaterials*, **26**, 599 (2005).